Journal of Atmospheric Chemistry **42:** 323–357, 2002.

Chemical Mechanism Development: Laboratory Studies and Model Applications

HARALD GEIGER [1], IAN BARNES [1], KARL H. BECKER [1], BIRGER BOHN [2], THEO BRAUERS [3], BIRGIT DONNER [1], HANS-PETER DORN [3], MANFRED ELEND [2], CARLOS M. FREITAS DINIS [1], DIRK GROSSMANN [4], HEINZ HASS [5], HOLGER HEIN [6], AXEL HOFFMANN [6], LARS HOPPE [3], FRANK HÜLSEMANN [3], DIETER KLEY [3], BJÖRN KLOTZ [7], HANS G. LIBUDA [8], TOBIAS MAURER [1], DJURO MIHELCIC [3], GEERT K. MOORTGAT [4], ROMEO OLARIU [1], PETER NEEB [4], DIRK POPPE [3], LARS RUPPERT [9], CLAUDIA G. SAUER [1], OLEG SHESTAKOV [8], HOLGER SOMNITZ [6], WILLIAM R. STOCKWELL [10], LARS P. THÜNER [1], ANDREAS WAHNER [3], PETER WIESEN [1], FRIEDHELM ZABEL [8], REINHARD ZELLNER [6] and CORNELIUS ZETZSCH [2]

[1] *Bergische Universität GH Wuppertal, FB 9 – Physikalische Chemie, D-42097 Wuppertal, Germany, e-mail: geiger@physchem.uni-wuppertal.de*
[2] *Fraunhofer-Institut für Toxikologie und Aerosolforschung, Physikalische Chemie, Nikolai-Fuchs-Straße 1, D-30625 Hannover, Germany*
[3] *Forschungszentrum Jülich GmbH, Stetternicher Staatsforst, D-52425 Jülich, Germany*
[4] *Max-Planck-Institut für Chemie, Chemie der Atmosphäre, Postfach 3060, D-55020 Mainz, Germany*
[5] *FORD-Forschungszentrum Aachen GmbH, Süsterfeldstraße 200, D-52072 Aachen, Germany*
[6] *Universität GH Essen, Institut für Physikalische und Theoretische Chemie, Universitätsstraße 5, D-45117 Essen, Germany*
[7] *National Institute for Environmental Studies, Atmospheric Environment Division, 16-2 Onogawa, Tsukuba, Ibaraki 305-0051, Japan*
[8] *Universität Stuttgart, Institut für Physikalische Chemie, Pfaffenwaldring 55, D-70569 Stuttgart, Germany*
[9] *Fraunhofer-Institut für Atmosphärische Umweltforschung, Kreuzeckbahnstraße 19, D-82467 Garmisch-Partenkirchen, Germany*
[10] *Desert Research Institute, Division of Atmospheric Sciences, 22 Raggio Parkway, Reno, NV 89512-1095, U.S.A.*

(Received: 15 August 2000; accepted: 22 December 2000)

Abstract. Within the German Tropospheric Research Programme (TFS) numerous kinetic and mechanistic studies on the tropospheric reaction/degradation of the following reactants were carried out:

- oxygenated VOC,
- aromatic VOC,
- biogenic VOC,
- short-lived intermediates, such as alkoxy and alkylperoxy radicals.

At the conception of the projects these selected groups were classes of VOC or intermediates for which the atmospheric oxidation mechanisms were either poorly characterised or totally unknown. The motivation for these studies was the attainment of significant improvements in our understanding of the atmospheric chemical oxidation processes of these compounds, particularly with respect to their involvement in photooxidant formation in the troposphere.

In the present paper the types of experimental investigations performed and the results obtained within the various projects are briefly summarised. The major achievements are highlighted and discussed in terms of their contribution to improving our understanding of the chemical processes controlling photosmog formation in the troposphere.

Key words: chemical mechansisms, boxmodel, laboratory studies, smog chamber, tropospheric chemistry.

1. Introduction

A fundamental goal of the German Tropospheric Research Programme (TFS) was the improvement of knowledge about chemical processes related to the formation of photooxidants in the troposphere. This knowledge is directly applied in the chemical modules used in chemistry and transport models (CTM). Existing chemical mechanisms designed for that purpose, e.g., the regional atmospheric chemistry mechanism, RACM (Stockwell *et al.*, 1997), or the RADM2 model (Stockwell *et al.*, 1990), which is still one of the chemical modules most frequently used in CT modelling in Europe, often do not incorporate actual kinetic and mechanistic data. The description of the degradation of aromatic and biogenic VOC, in particular, is one of the most important and also weakest aspects of the models, which requires extensive improvement. In addition, a large number of oxygenated VOC are expected to gain importance in tropospheric chemistry in the near future. These compounds, which are anticipated to improve air quality, are likely to find increased use as alternative solvents or fuel additives because of environmental legislation by National Governments and the EU. At present, most classes of oxygenated VOC are not appropriately represented in currently established chemical models.

The TFS programme included a group of projects, designed to better characterise the tropospheric behaviour of oxygenated, aromatic and biogenic VOC in laboratory and outdoor chamber studies. In addition, experimental studies on intermediates occurring in the tropospheric degradation of VOC, e.g., alkoxy and alkylperoxy radicals, were also performed. Based on the data obtained from the experiments, tropospheric degradation mechanisms of selected compounds have been considerably improved or established for the first time. The major results are outlined below.

The final outcome of these investigations will be an improved chemical mechanism for application in CT modelling studies related to ozone prognosis and abatement strategies.

2. Experimental and Modelling Details

Due to the nature of the present paper, it is not possible to describe in detail all the experimental techniques and facilities employed in the various studies. Nevertheless, in order to give a broad overview of the experimental approaches, the different set-ups used in the investigations are briefly cited below.

2.1. EXPERIMENTAL TECHNIQUES

Bimolecular rate coefficients for the reactions of OH radicals with a number of aromatic, oxygenated and biogenic VOC were obtained using either the relative rate technique (Sauer *et al.*, 1999a) or the absolute method (Becker *et al.*, 1999a, b). For the former technique, measurements of the decay of VOC concentrations relative to a reference compound in a static photoreactor were performed. The latter method uses the time-dependent measurement of the relative OH radical concentration by laser-induced fluorescence in a flow tube system.

In a couple of additional kinetic experiments related to aromatic VOC, OH radicals were measured as function of reaction time using resonance fluorescence (Knispel *et al.*, 1990) or cw-UV laser long-path absorption (Bohn *et al.*, 1999).

Product studies on the OH-initiated oxidation of selected VOC were performed in photoreactor experiments. Generally, mixtures of VOC, NO_x, air and an OH-radical precursor (photolysis of CH_3ONO, HONO or H_2O_2) were irradiated by natural or artificial light sources in suitable reaction chambers, either in a 1000 l quartz glass laboratory reactor (Barnes *et al.*, 1994) or in the European Photoreactor EUPHORE in Valencia, Spain. A detailed description of this outdoor facility is given in Becker (1996) and Barnes and Wenger (1998). Time-resolved concentrations of reactants and reaction products were determined by means of long-path FTIR spectroscopy or gas chromatography (e.g., Sauer *et al.*, 1999a, Thüner *et al.*, 1999).

Rate coefficients for the reactions of a series of alkoxy radicals with O_2 and for their thermal decomposition or isomerisation were obtained using photolytic generation of alkyl radicals in the presence of O_2/NO combined with simultaneous detection of NO_2 and OH concentration-time profiles. From these profiles, rate coefficients were derived by numerical simulation using an explicit chemical mechanism. Details of this experimental arrangement can be found in Hoffmann *et al.* (1992).

A series of experiments on the atmospheric fate of selected alkoxy radicals were performed in a temperature-controlled quartz photoreactor ($v = 200$ l, Libuda *et al.*, 2000). Alkoxy radicals, RO, were generated by cw photolysis of the corresponding iodides, RI, in the presence of O_2 and NO, using N_2 as buffer gas. Rate coefficient ratios of the competing reactions of RO, i.e., unimolecular decay or isomerisation versus reaction with O_2, were derived from the product distributions, which were obtained by long-path IR absorption using an FT-IR spectrometer.

The experiments related to the degradation of 2-butylperoxy radicals were carried out in a flow system, in which the peroxy radicals were produced *in situ* in a mixture of VOC, NO, N_2 and O_2. OH radicals were produced by photolysis of HCHO. The O_2 mixing ratio was kept low so that the radicals as well as their decomposition and isomerisation products were transformed into alkyl nitrates and nitrites by reaction with the excess NO in the system. After cryogenic preconcentration, the products were separated by gas chromatography and detected after conversion to NO by a chemiluminescence detector.

Ozonolysis experiments were carried out in a static reactor in the absence and presence of water vapour, with reactant concentrations in the low ppm range. Products were analysed with a combination of long-path FTIR spectroscopy, GC-FID and HPLC. H_2O_2 and organic hydroperoxides were collected using a coil collector and detected using peroxidase-catalysed decomposition in the presence of *p*-hydroxyphenyl acetic acid and fluorescence detection of the biphenyl derivate. Further details can found in Sauer *et al.* (1999b) and Grossmann (1999).

A number of experiments with respect to the influence of biogenic VOC on tropospheric ozone formation were carried out in the European Photoreactor in Valencia, Spain.

2.2. MODELLING TECHNIQUES

The computer simulations related to oxygenated and aromatic VOC degradation mechanisms were carried out using the box model SBOX (Seefeld and Stockwell, 1999). This FORTRAN programme incorporating the Gear algorithm (Gear, 1971) was operated either on an SGI Origin 200 workstation running under IRIX 6.5 or on a SUN Sparc Station with SunOS 5.5.1. The programme uses the public domain library VODE (Brown *et al.*, 1989) to integrate the ordinary differential equations. Other box model calculations were performed using the commercial programme package FACSIMILE (AEA Technology).

3. Results and Discussion

3.1. TROPOSPHERIC OXIDATION OF OXYGENATED VOC

Oxygenated compounds such as specific ethers and diethers are either currently in use or are being considered as gasoline/diesel fuel additives and solvents. For example, fuel reformulation by addition of methyl *tert*-butyl ether leads to a significant reduction of carbon monoxide and hydrocarbons in the exhaust gas and increases the octane number. In addition, it has been shown that the partial replacement of aromatic VOC in gasoline fuels by oxygenated VOC leads to a significant reduction of the ozone formation potential of exhaust gases and therefore should diminish tropospheric ozone formation resulting from automobile exhaust (Becker, 1998).

Diethers and acetals are currently under discussion as potential additives to diesel for the reduction of particle emissions. The increased employment of oxygenated VOC inevitably results in increased emissions into the atmosphere. The major sink of these compounds in the troposphere is reaction with OH radicals. Consequently, an accurate knowledge of the kinetics and degradation reaction pathways of the OH-initiated oxidation of oxygenated VOC is a prerequisite for a reliable estimation of the effect of these compounds on photosmog formation.

3.1.1. *Experimental Studies*

Bimolecular rate coefficients for the reactions of atmospherically relevant oxygenated VOC with OH radicals and Cl atoms were obtained. The experiments were performed at 298 ± 2 K using either the relative rate (RR) technique in 760 Torr air or the laser photolysis/laser-induced fluorescence (LP/LIF) method in argon in the pressure range 50–400 Torr. The reactions studied by LP/LIF showed no pressure dependence within the range investigated. The rate coefficients obtained are summarised in Table I.

Product studies of the reactions of OH radicals with selected oxygenated VOC in 760 Torr air were carried out in the presence of NO_x. Three different types of ethers were examined: monoethers, ethylene glycol ethers and formaldehyde acetals (see Table II). The main oxidation products of the OH-initiated oxidation of all these compounds are formates. Minor products of the gas-phase oxidation of formaldehyde acetals are carbonates and aldehydes. The three main oxidation products of each compound investigated in the presence of NO_x are listed in Table II together with their molar yields.

Photolysis studies on the formates and carbonates given in Table II showed that under tropospheric conditions, the photolysis of these compounds is negligible. In addition, as shown in Table II, the OH reactivities of formates and carbonates are significantly lower than those of their precursors. On the other hand, all esters, formates and carbonates as well as a large number of formaldehyde acetals are highly soluble in water, which will facilitate the removal of these species from the troposphere by wet deposition. However, the transport of esters and acetals from the urban sources to remote areas might play a role. From the observed laboratory behaviour it can be concluded, that the contribution of the oxygenated VOCs, which are oxidised to formates and carbonates, to photosmog formation will probably be low. However, oxidation of some oxygenated organics investigated leads to high aldehyde yields, e.g., all di-*n*-alkoxy methanes except dimethoxy methane (see Table II). Due to the high photolysis frequencies of aldehydes in the troposphere and their large contribution to the radical budget, the air quality benefits gained by the widespread use of such oxygenated VOCs needs to be carefully weighed against the potential negative effects caused by the accompanying increase in aldehyde production.

Table I. Bimolecular rate coefficients for the reactions of OH radicals and Cl atoms with selected oxygenated VOC at room temperature and atmospheric pressure. The LP/LIF measurements were carried out in the range 50–400 Torr. None of these reactions was found to be dependent on total pressure

Reactant	k_{OH} (10^{-12} cm^3 s^{-1})	$k_{Cl}W$ (10^{-11} cm^3 s^{-1})	Method [a]	Reference
dimethoxy ethane	(27.0 ± 1.0)	–	RR	Barnes and Donner, 2000
1,4-dioxane	(12.4 ± 0.4)	–	RR	Maurer *et al.*, 1999
dimethoxy methane	(4.89 ± 0.19)	(14.1 ± 1.4)	RR	Thüner *et al.*, 1999
diethoxy methane	(18.4 ± 1.6)	–	RR	Thüner *et al.*, 1999
di-*n*-propoxy methane	(26.3 ± 4.9)	–	RR	Thüner *et al.*, 1999
di-*i*-propoxy methane	(34.7 ± 2.0)	–	LP/LIF	Becker *et al.*, 1999a
di-*n*-butoxy methane	(34.7 ± 4.2)	–	RR	Thüner *et al.*, 1999
	(33.9 ± 4.6)	–	LP/LIF	Becker *et al.*, 1999b
di-*sec*-butoxy methane	(42.5 ± 1.3)	–	LP/LIF	Becker *et al.*, 1999a
1,3-dioxolane	(10.4 ± 1.6)	(16.2 ± 1.5)	RR	Sauer *et al.*, 1999a
1,3,5-trioxane	(6.42 ± 0.61)	(9.56 ± 0.51)	RR	Platz *et al.*, 1998
methoxy ethyl formate	(5.12 ± 1.60)	–	RR	Barnes and Donner, 2000
methoxy methyl formate	(1.33 ± 0.16)	(3.38 ± 0.17)	RR	Hass, 2000
ethoxy methyl formate	(3.71 ± 0.22)	–	RR	Barnes and Donner, 2000
n-butoxy methyl formate	(8.00 ± 0.07)	–	RR	Barnes and Donner, 2000
methylene diformate	–	(0.056 ± 0.004)	RR	Sauer *et al.*, 1999a
ethylene diformate	(0.477 ± 0.061)	(0.35 ± 0.01)	RR	Maurer *et al.*, 1999
di-*n*-butyl carbonate	(7.07 ± 1.20)	–	RR	Barnes and Donner, 2000
diethyl carbonate	(1.79 ± 0.10)	–	RR	Barnes and Donner, 2000
dimethyl carbonate	(0.378 ± 0.084)	(0.204 ± 0.042)	RR	Hass, 2000
ethylene carbonate	≤ 0.1	(0.534 ± 0.080)	RR	Sauer *et al.*, 1999a

[a] RR: Relative Rate Technique; LP/LIF: Laser Photolysis/Laser-Induced Fluorescence.

3.1.2. *Chemical Modelling*

Explicit reaction mechanisms for the OH-initiated degradation of selected oxygenated VOC in the presence of NO_x were developed using a simple box model. Table III summarises the compounds investigated within TFS/LT3. The reaction schemes developed were optimised by fitting the model to the experimental concentration-time profiles for selected reactants, commonly the reactants, primary products, NO_x and O_3. The simulations were focused on indoor photoreactor experiments using methyl nitrite photolysis as the precursor for OH radicals.

The reactions describing the inorganic chemistry of the systems investigated as well as the photolysis reactions were taken from the RACM mechanism of Stockwell *et al.* (1997). The NO_2 and CH_3ONO photolysis frequencies were taken from comparable measurements in the photoreactor. All other photolysis frequencies were calculated relative to J_{NO_2} using the algorithm of Madronich (1987).

Figure 1 shows, as an example, the degradation mechanism for 1,3-dioxolane in the presence of NO_x. The given branching ratios were obtained by chemical mod-

Table II. Main primary reaction products of the OH-initiated oxidation of selected oxygenated VOC in air in the presence of NO_x. The molar yields are given in parentheses

Reactant	Product 1	Product 2	Product 3	Reference
ethyl-*tert*-butyl ether	*tert*-butyl formate (60–70%)	*tert*-butyl acetate (15–20%)	acetone (2–8%)	Barnes and Donner, 2000
methyl-*tert*-butyl ether	*tert*-butyl formate (60–70%)	formaldehyde (10–30%)	methyl acetate (10–20%)	Barnes and Donner, 2000
dimethoxy ethane	methyl formate (180 ± 18%)	methoxy ethyl formate (15 ± 2%)	–	Barnes and Donner, 2000
1,4-dioxane	ethylene diformate (94 ± 10%)	–	–	Maurer *et al.*, 1999
dimethoxy methane	methoxy methyl formate (71 ± 7%)	dimethyl carbonate (26 ± 2%)	methyl formate (4 ± 2%)	Hass, 2000
diethoxy methane	ethoxy methyl formate (65 ± 13%)	formaldehyde (80 ± 16%)	acetaldehyde (32 ± 4%) *W*	Barnes and Donner, 2000
di-*n*-propoxy methane	*n*-propoxy methyl formate (66 ± 13%)	acetaldehyde (81 ± 16%)	di-*n*-propyl carbonate ≤ 7%	Barnes and Donner, 2000
di-*n*-butoxy methane	*n*-butoxy methyl formate (77 ± 15%)	propionaldehyde (78 ± 16%)	di-*n*-butyl carbonate ≤ 10%	Maurer *et al.*, 2000
1,3-dioxolane	methylene diformate (52 ± 3%)	ethylene carbonate (47 ± 8%)	–	Sauer *et al.*, 1999a
1,3,5-trioxane	methylene diformate (100 ± 5%)	–	–	Platz *et al.*, 1998

Table III. Oxygenated VOC investigated on which the chemical modelling work in TFS/LT3 was focused. For these compounds, explicit OH-initiated degradation mechanisms in the presence of NO_x were developed

Class of compound	VOC	Reference
aliphatic diethers	dimethoxy methane	Geiger and Becker (1999)
	dimethoxy ethane	Geiger and Becker (1999)
	di-*n*-butoxy methane	Maurer *et al.* (2000)
cyclic diethers	1,4-dioxane	Geiger *et al.* (1999)
	1,3-dioxolane	Sauer *et al.* (1999a)

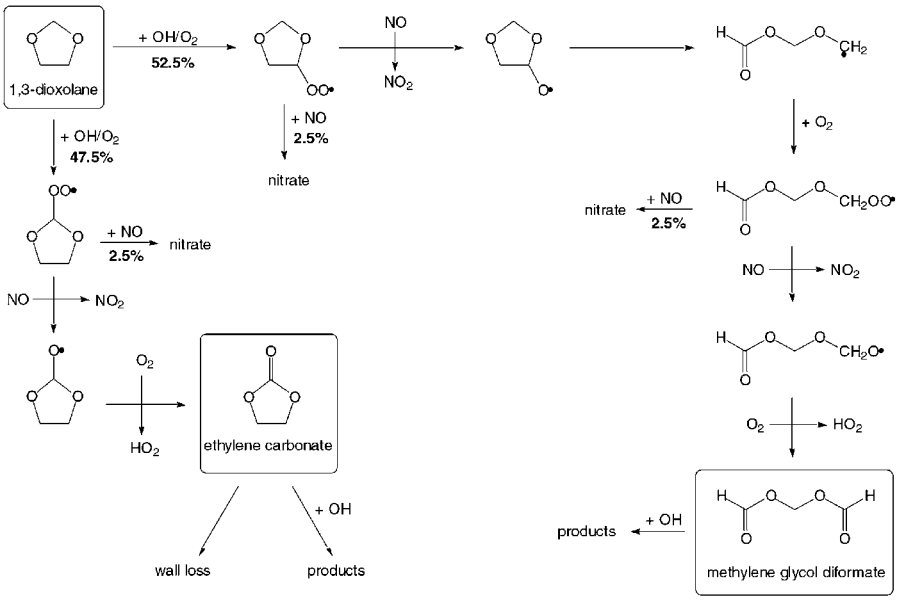

Figure 1. Reaction scheme for the OH-initiated degradation of 1,3-dioxolane in the presence of NO_x.

elling. Figure 2 illustrates the excellent agreement obtained between measured and simulated concentration-time profiles for a typical photoreactor experiment. The results for the modelling studies related to the other oxygenated VOC summarised in Table III are not shown here in detail. For these studies, the simulations are of similar high quality.

An assessment of the influence of oxygenated VOC on tropospheric photochemistry has been made by using a chemical box model and taking dimethoxy methane (DMM) as an example. For this purpose, the condensed RACM mechanism (Stockwell *et al.*, 1997), expanded by the explicit dimethoxy methane chemistry (Geiger and Becker, 1999), was used to simulate a set of typical urban and sub-urban

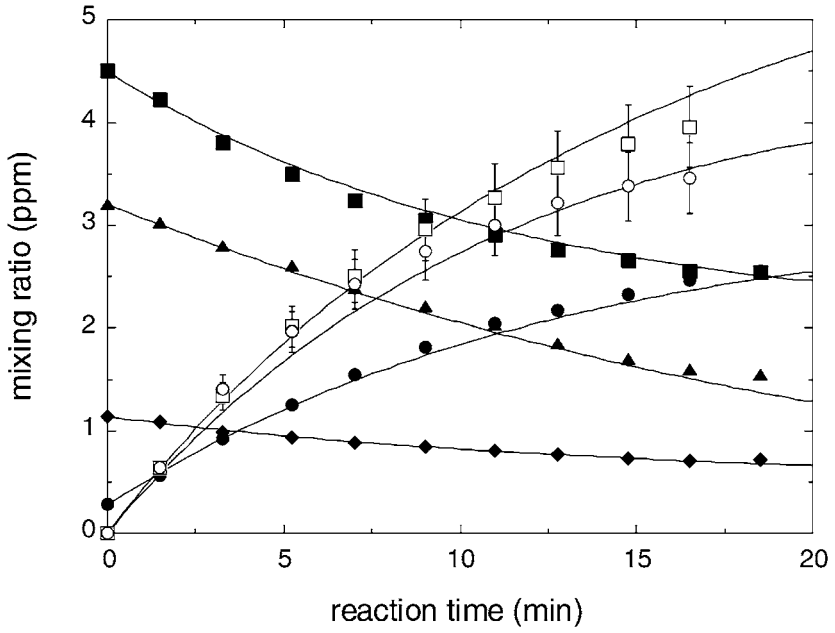

Figure 2. Comparison of experimental (symbols) and simulated (curves) concentration-time profiles: 1,3-dioxolane (♦), CH_3ONO (▲), NO (■), NO_2 (●), ethylene carbonate × 20 (○) and methylene glycol diformate × 20 (□). Error bars are only shown for the primary products. Initial mixing ratios (ppm): 1,3-dioxolane (1.14), NO (4.50), NO_2 (0.28) and CH_3ONO (3.20) in 760 Torr air at 298 ± 2 K.

scenarios. The procedure was designed to determine the relative reactivities of VOC and dimethoxy methane for multiple day periods. Single day scenarios are typically used to calculate incremental reactivities. However, this procedure may not give a complete picture since less reactive compounds have a long residence time in the atmosphere. Another important consideration is that the concentration of their oxidation products may build up over a multiple day period. Therefore, single day simulations may underestimate, for example, the reactivity of ethane. The maximum ozone incremental reactivity and maximum incremental reactivities scenarios were determined for time periods from one to six days. Details are given in Stockwell *et al.* (2001).

The simulation results were used to calculate ozone formation potentials as maximum ozone incremental reactivities (MOIR) and maximum incremental reactivities (MIR, Carter, 1994). It was found that the change in ozone production was linear with respect to the changes in the emission rates for ethane and dimethoxy methane for the conditions employed, as demonstrated in Figure 3. The MOIR and MIR values increased for ethane and dimethoxy methane as the level of pollution and the length of the simulation was increased but the MIOR and MIR values of ethane increased faster than those for dimethoxy methane. On this basis, dimethoxy methane has an ozone forming potential on a per mass basis that is only somewhat

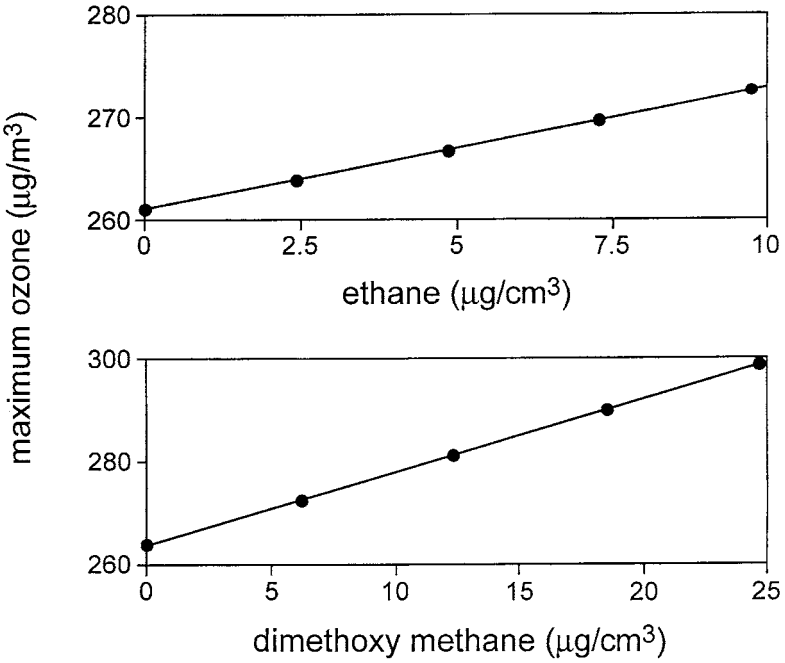

Figure 3. MIR calculations for ethane and dimethyoxymethane. The maximum ozone concentrations were plotted as functions of the total VOC emissions for the 5 day MIR scenario.

greater than that of ethane if scenarios for multiple days are considered. The results show that reactivity should be evaluated by calculations involving multiple day scenarios.

3.1.3. *Conclusions*

Laboratory and model studies within the TFS/LT3 suggest that the partial replacement of aromatic VOC in gasoline fuels by oxygenated VOC should lead to a significant reduction of tropospheric ozone formation resulting from automobile exhaust gases. The same observation is valid for solvents, where aromatic hydrocarbons are widely used. It can be concluded from the results of the project that particularly those oxygenated additives or substitutes, which are oxidised to low reactive degradation products, might be highly effective for the reduction of ozone formation. Accordingly, compounds yielding photochemically unstable aldehydes (e.g., see Table II) should not be used as additives or surrogates. Structure activity studies based on present results now allow the estimation of the suitability of the oxygenated VOCs investigated as additives or substitutes with respect to tropospheric ozone formation.

3.2. TROPOSPHERIC OXIDATION OF AROMATIC VOC

On the basis of model calculations aromatic hydrocarbons, mainly BTX (benzene, toluene and the xylene isomers), are predicted to contribute up to as much as 40% to the formation of O_3 and other photooxidants in urban areas (Derwent *et al.*, 1998). However, the reliability of these predictions is very much dependent on the accuracy of the degradation mechanisms utilised in the chemistry modules incorporated into chemistry-transport models (CTM). The modules, which were currently in use at the conception of the TFS project, contained many speculative kinetic and mechanistic elements. Consequently extensive efforts were made within the framework of the TFS research project to elucidate the aromatic hydrocarbon photo-oxidation mechanisms.

Reaction with OH radicals dominates the tropospheric oxidation processes of aromatic hydrocarbons. The reactions proceed by (i) OH radical addition to the aromatic ring to form a hydroxycyclohexadienyl radical, i.e., an OH-aromatic-adduct, which can thermally decompose back to reactants or undergo further reactions to products and (ii) H-atom abstraction from one of the C–H bonds of alkyl substituent groups. The later process results in the formation of ring-retaining aromatic aldehyde products and accounts for $\leq$10% of the overall process (e.g., Atkinson, 2000). Subsequent reactions of the OH-aromatic-adducts are much more complex and various different mechanisms have been proposed to account for the observed products and experimental observations (Klotz *et al.*, 1997).

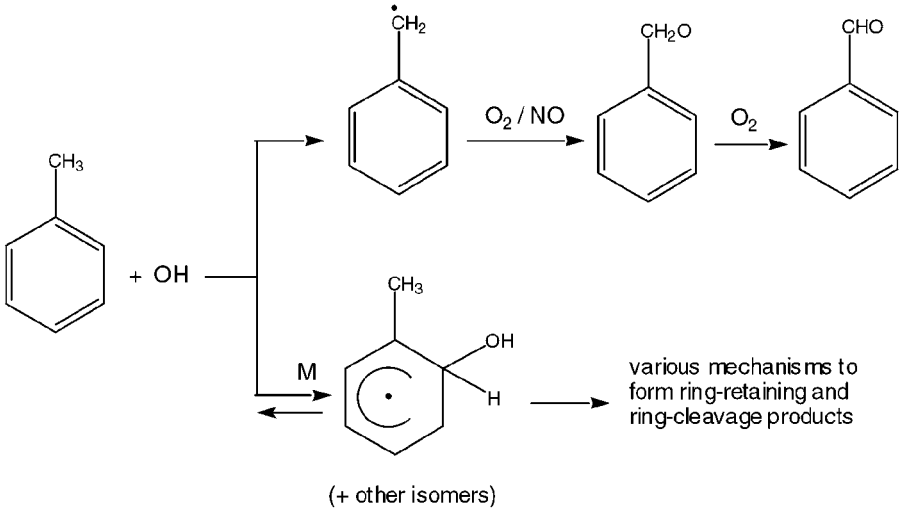

Work on the primary reaction steps for several OH-aromatic-adducts has been performed using long-path detection of both OH and the OH-adducts (Bohn and Zetzsch, 1999). Results obtained for benzene, toluene and toluene-d_8 are consistent with a reversible, peroxy-adduct-forming addition of O_2 to the OH-aromatic-

adduct with equilibrium constants of $(2.7 \pm 0.4) \times 10^{-19}$, $(3.3 \pm 0.3) \times 19^{-19}$ and $(3.1 \pm 1.2) \times 19^{-19}$ cm^3 for the OH-benzene, OH-toluene and OH-toluene-d_8 adducts, respectively. The reaction sequence is illustrated for toluene below.

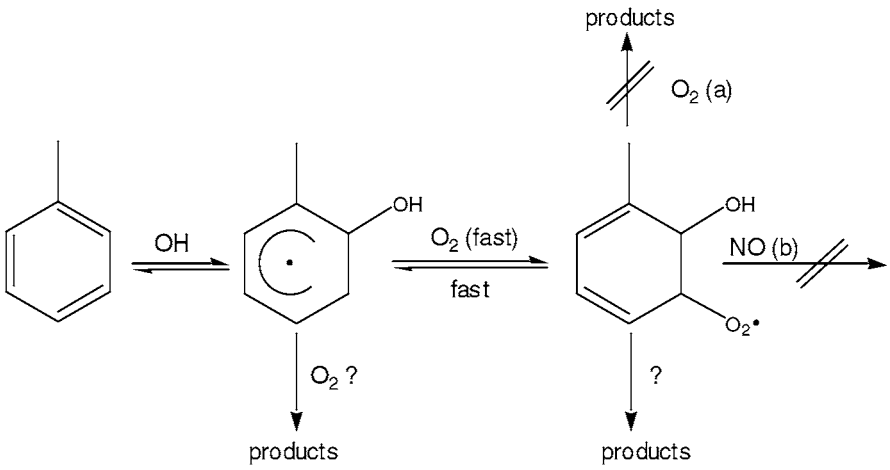

(a) < 10^{-17} cm^3 s^{-1}
(b) < 0.7% at 50 ppb NO (benzene: 1.7%)

From fits of the experimental data rate coefficients have been determined for the self-reaction of the OH-aromatic-adducts and their reaction with HO_2 radicals. The effective loss rate for both radical species in equilibrium, i.e., the OH-adduct and the OH-adduct-peroxy radical, was found to be of the order of 1 ms for toluene under tropospheric conditions compared to 2.5 ms in the case of benzene. Based on these lifetimes, the work supports that reactions of the adduct-peroxy-radicals with NO will not be significant under atmospheric conditions even if comparatively fast rate coefficients are assumed. This implies that the expected products of the reactions of NO with the adduct-peroxy-radicals, namely 2,4-hexadienedial-type compounds are unimportant in the atmosphere. However, under conditions where NO levels are significantly higher than in the troposphere, such as product studies under laboratory conditions, these reactions may be important.

Further reactions of the OH-aromatic-adducts can lead to ring-retaining or ring cleavage products. Phenolic compounds are major ring-retaining products formed by abstraction of a ring H-atom with O_2. Work was performed in the EUPHORE photoreactor on the quantification of phenol yield from the photooxidation of benzene and *o*-, *m*- and *p*-cresol from the photooxidation of toluene using *in situ* DOAS and FT-IR spectrometry. The work has helped to reduce the uncertainty concerning the cresol yields in the literature (Klotz *et al.*, 1998a). The studies also clearly demonstrated that NO_3 radical chemistry plays an important role in chamber simulation experiments and needs to be carefully considered in their

interpretation. This is also confirmed by field studies carried out in a German city, which indicate that the reactions of NO_3 with phenolic compounds also occur during daytime (Kurtenbach *et al.*, 2000).

A phenol yield of 50% has been observed from the photooxidation of benzene, which is twice as large as previously reported values. However, this result still requires validation using independent methods.

It has been postulated that reaction of the OH-aromatic-adducts with O_2 could also result in the formation of arene oxides (Klotz *et al.*, 1997), e.g., for toluene:

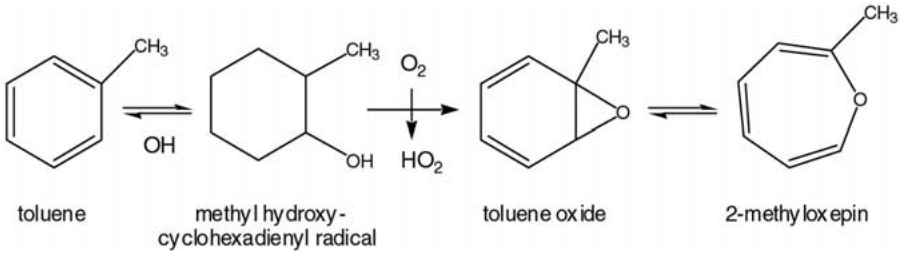

To prove or disprove this proposal, comprehensive studies were performed on the atmospheric chemistry of benzene oxide/oxepin and toluene-1,2-oxide/2-methyloxepin. These studies included measurements of photolysis frequencies, rate coefficients for reactions with OH and NO_3 radicals (see Tables IV–VI), and also product analyses (Klotz *et al.*, 1997, 1998b, 2000). However, it is presently still unclear whether arene oxides will be important in the oxidation mechanism of aromatic hydrocarbons; current experimental and theoretical evidence suggests that arene oxides may only be produced with minor yields.

Product studies have been performed on the reactions of OH and NO_3 radicals with phenol and the cresol isomers. It has been shown for the first time that reaction with OH leads to the formation of dihydroxybenzenes in high yield and nitrophenols and benzoquinones in relatively low yields. As observed in other studies (Atkinson, 1994), reaction with NO_3 was found to result predominantly in the formation of toxic nitrophenols. Rate coefficients have also been determined, for the first time, for the reaction of OH with a series of dihydroxybenzenes and benzoquinones. The rate coefficients for the dihydroxybenzenes are typically (1–2) $\times$ 10^{-10} cm^3 s^{-1} and those for the benzoquinones (2–5) $\times$ 10^{11} cm^3 s^{-1} (Olariu *et al.*, 2000).

The atmospheric chemistry of many known and postulated carbonyl ring-cleavage products has also been investigated. This work included kinetic and product studies of the OH and NO_3 radical reactions with hexadienedials and butenals. The photolytic properties of these compounds and some α-dicarbonyls have also been studied under natural sunlight conditions. Tables IV–VI summarise some of the new kinetic and photolytic data obtained within the TFS programme. Details of the investigations can be found in the listed publications.

Table IV. Summary of OH and NO_3 kinetic data for aromatic compounds and oxidation products investigated within the TFS/LT3 programme

Reaction	k (298 K) ($cm^3\ s^{-1}$)	Reference
OH + benzene → products	$(1.10 \pm 0.07) \times 10^{-12}$ (N_2) $(1.06 \pm 0.07) \times 10^{-12}$ (O_2)	Bohn and Zetsch, 1999
OH + toluene → products	$(5.7 \pm 0.2) \times 10^{-12}$ (N_2) $(5.6 \pm 0.14) \times 10^{-12}$ (O_2)	Bohn *et al.*, 2000
OH + toluene-d_8 → products	$(5.3 \pm 0.3) \times 10^{-12}$ (N_2) $(5.47 \pm 0.14) \times 10^{-12}$ (O_2)	Bohn *et al.*, 2000
OH + glycidaldehyde → products	$(1.69 \pm 0.04) \times 10^{-11}$	Ma *et al.*, 1998
OH + benzene oxide/oxepin → products	$(10.0 \pm 0.4) \times 10^{-11}$	Klotz *et al.*, 1997
OH + toluene oxide/2-methyloxepin → products	$(2.1 \pm 0.1) \times 10^{-10}$	Klotz *et al.*, 2000
OH + E,Z-2,4-hexadienedial → products	$(7.4 \pm 1.9) \times 10^{-11}$	Klotz *et al.*, 1999
OH + E,E-2,4-hexadienedial → products	$(7.6 \pm 0.8) \times 10^{-11}$	Klotz *et al.*, 1999
NO_3 + benzene oxide/oxepin → products	$(9.2 \pm 0.3) \times 10^{-12}$	Klotz *et al.*, 1997
NO_3 + toluene oxide/2-methyloxepin → products	$(1.27 \pm 0.10) \times 10^{-11}$	Klotz *et al.*, 2000

Table V. Kinetic data for the reaction of OH with trimethylbenzene isomers obtained within the TFS/LT3 programme

Reaction	$k(T)$ 10^{-11} (cm^3 s^{-1})		k (298 K) (cm^3 s^{-1})
OH + 1,2,3-trimethylbenzene → products	$3.7–5.9 \times 10^3 \exp(-2650\ K/T)$	(277–298 K)	2.93×10^{-11}
	$2.5 \times 10^{-2} \exp(1420\ K/T)$	(298–339 K)	
OH + 1,2,4-trimethylbenzene → products	$3.9–1.6 \times 10^{12} \exp(-8450\ K/T)$	(272–298 K)	3.15×10^{-11}
	$6.7 \times 10^{-4} \exp(2520\ K/T)$	(298–338 K)	
OH + 1,3,5-trimethylbenzene → products	$0.63 \exp(670\ K/T)–1.2 \times 10^{12} \exp(-9400\ K/T)$	(275–342 K)	5.94×10^{-11}

Table VI. Summary of photolysis frequency data obtained for aromatic hydrocarbon oxidation products

Reaction	Photolysis frequency data (298 K)	Reference
glycidaldehyde + $h\nu \rightarrow$ products	$J(h\nu) = 1.0 \times 10^{-4}$ s^{-1} (1 July, noon, and 50° N, assumed quantum yield of 1) [a]	Ma *et al.*, 1998
benzene oxide/oxepin + $h\nu \rightarrow$ products	$J(\text{benzeneoxide/oxepin})/J(NO_2) = (4.41 \pm 0.44) \times 10^{-2}$ [b]	Klotz *et al.*, 1997
toluene oxide/2-methyloxepin + $h\nu \rightarrow$ products	$J(\text{tolueneoxide/methyloxepin})/J(NO_2) = (3.99 \pm 0.48) \times 10^{-2}$ [b]	Klotz *et al.*, 2001
E,Z-2,4-hexadienedial + $h\nu \rightarrow$ products	Rapid photoisomerization of E,Z-2,4-hexadienedial to E,E-2,4-hexadienedial	Klotz *et al.*, 1999
	$J(\text{E,Z-2,4-hexadienedial})/J(NO_2) = (0.148 \pm 0.012)$ [b, c]	
E,E-2,4-hexadienedial + $h\nu \rightarrow$ products	$J(\text{E,Z-2,4-hexadienedial}) \rightarrow \text{EQUI})/J(NO_2) = (0.113 \pm 0.009)$	Klotz *et al.*, 1999
	$J(\text{EQUI} \rightarrow \text{E,Z-2,4-hexadienedial})/J(NO_2) = (0.192 \pm 0.016)$	
	K (equilibrium) $= (0.59 \pm 0.07)$	
	$J(\text{E,E-2,4-hexadienedial}) \rightarrow \text{products})/J(NO_2) = J(\text{EQUI} \rightarrow \text{products})/J(NO_2) = (1.22 \pm 0.45) \times 10^{-2}$ [b, d]	
glyoxal + $h\nu \rightarrow$ products	$J(\text{glyoxal})/J(NO_2) = (0.0105)$ [b]	Klotz *et al.*, 2001
methylglyoxal + $h\nu \rightarrow$ products	data uncertain, see reference	Klotz *et al.*, 2001
biacetyl + $h\nu \rightarrow$ products	$J(\text{biacetyl})/J(NO_2) = (0.0364 \pm 0.0026)$ [b]	Klotz *et al.*, 2001

[a] J estimated from UV spectrum.
[b] J(compound) measured relative to $J(NO_2)$ in the EUPHORE photoreactor under natural sunlight conditions.
[c] Rapid photoisomerization of E,Z-2,4-hexadienedial to E,E-2,4-hexadienedial.
[d] Complex photolysis behaviour observed, a fast equilibrium is preceded by comparably slow photolysis loss. Processes can be described by the given equations.

Although much new and encouraging information concerning the mechanisms of the atmospheric oxidation of aromatic hydrocarbons emerged from the TFS project, vital information concerning the actual nature of the ring-opening process which is necessary for realistic model construction is still uncertain.

3.2.1. *Conclusions*

In conclusion, the work on the primary reaction steps of the aromatic hydrocarbons has shown quite distinctly that the OH-aromatic adduct-peroxy radicals will not react with NO under atmospheric conditions. This correlates well with end-product studies where little difference was observed in the product distribution with and without NO_x in the system. The results also indicate that formation of arene oxides is probably not an important initial reaction pathway, however, the actual importance still needs to be quantified. Much new mechanistic information has been obtained on ring-cleavage products, which will enable immensely improve the description of the chemistry of these species in the models.

The yields of phenolic ring-retaining products have been determined with high precision. It has been shown for the first time that further reaction of the phenolic compounds with OH results predominantly in the formation of dihydroxybenzenes. In agreement with other studies, reaction with NO_3 was found to produce mainly nitrophenols. The results are in agreement with field measurements of the *p*-cresol/toluene ratio made in a German city, which indicate that reactions of NO_3 with phenolic compounds also occur during daytime. Since toxic nitrophenols are formed in these reactions, more detailed studies on the sources and atmospheric of chemistry phenols should be a future research priority.

3.3. TROPOSPHERIC OXIDATION OF BIOGENIC VOC

The chemistry of biogenic hydrocarbons adds a considerable amount of uncertainty to tropospheric chemistry models. Whereas the chemistry of isoprene oxidation has been incorporated into most chemistry models, it was only very recently that schemes for the oxidation of terpenes became available both in compressed form (RACM, Stockwell *et al.*, 1997) and in form of an explicit mechanism (Master Chemical Mechanism, MCM, Jenkin *et al.*, 1997). Since the chemical nature of biogenic hydrocarbons is very diverse and detailed oxidation schemes are far too complicated to be used in most applications, some kind of simplification ('lumping') is necessary. In general, chemical lumping can be made by two different approaches:

- Intermediate radicals (mostly peroxy radicals) are not explicitly treated and reactions are expressed in a way that only stable products are formed as a result of a specific oxidation step. This procedure obviously underestimates the radical production as well as the ozone formation.

- Another approach to reduction in reaction complexity is to group the stable products and radical intermediates into a limited number of classes which is normally equivalent to a 'downsizing' of the products.

The latter approach is used in the RACM mechanism by Stockwell *et al.* (1997) that will be discussed in the following section due to its wide acceptance as a chemical module for CT model applications.

3.3.1. *Ozonolysis Reactions*

In order to represent ozone-alkene reactions in a manner suitable for tropospheric modelling the following approach has been developed: Following the initial addition of the ozone molecule to the double bond a carbonyl compound and a Criegee intermediate (CI) is formed.

$$R_2C{=}CR_2 + O_3 \rightarrow \text{primary ozonide} \qquad \text{(R1)}$$

$$\text{primary ozonide} \rightarrow R_2COO^* + R_2CO\,. \qquad \text{(R2)}$$

In analogy to the reactions of CI in the aqueous phase, it is commonly accepted that essentially three pathways exist (Atkinson, 2000, Calvert *et al.*, 2000). Other pathways have been discussed but only for specific alkenes and with a relative yield of less than 5%. Two of the pathways lead to the decomposition of the exited CI, whereas the third pathway forms, after collisional stabilisation, the 'stabilised CI', which can undergo reactions with atmospheric trace gases.

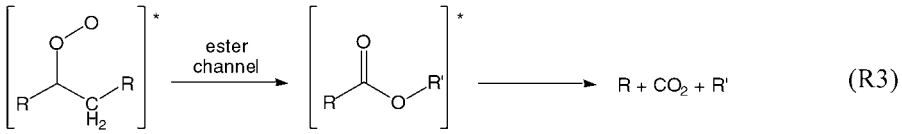

(R3)

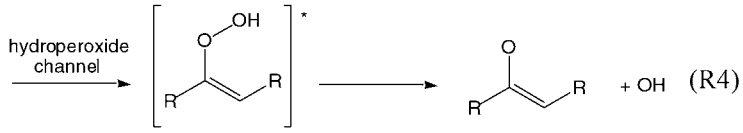

(R4)

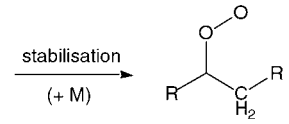

(R5)

For both the hydroperoxide (R4) and the stabilisation (R5) channel, several specific products exist, which can be used as reaction tracers. Hence, the relative importance of the Reactions (3)–(5) can be experimentally assessed, which is helpful for

the development of mechanisms. For the hydroperoxide channel the tracer molecule is the OH radical. Its formation yield has been measured for most alkenes (Paulson, 1999, Rickard *et al.*, 1999, Calvert *et al.*, 2000). The extent of stabilisation is known for a limited number of alkenes from the study of Hatekeyama *et al.* (1984) and from a more extensive experimental investigation using the formation of H_2O_2 and hydroxyalkylhydroperoxides ($R_2C(OH)OOH$) from the reaction of the stabilised Criegee intermediate with water vapour (Becker *et al.*, 1990, 1993; Thamm *et al.*, 1996; Neeb *et al.* 1997; Sauer *et al.*, 1999b; Grossmann, 1999; Bauerle and Moortgat, 1999; Grossmann *et al.*, 2000):

$$R_2COO + H_2O \rightarrow R_2CO + H_2O_2 \quad \text{(R6a)}$$

$$\rightarrow R_2C(OH)OOH\,. \quad \text{(R6b)}$$

It should be noted that under atmospheric conditions the fate of the stabilised CI is reaction with water vapour, Reaction (R6). Under laboratory conditions, a variety of other product channels have been observed (Neeb *et al.*, 1996, 1998). As expected from the kinetics of Reactions (R3)–(R6), the OH radical formation yield shows a negative correlation with the degree of stabilisation as determined from measured H_2O_2 (and H_2SO_4) yields (see Figure 4, Grossmann, 1999). Yields for stabilisation (Y_{stab}) and OH radical formation (Y_{OH}) can be directly used for the development of individual alkene and terpene oxidation schemes for condensed chemical models (e.g., the RACM mechanism, Stockwell *et al.*, 1997), as exemplified below for 2,3-dimethyl-2-butene (Neeb and Moortgat, 1999):

$$\begin{aligned}(CH_3)_2C{=}C(CH_3)_2 + O_3 \rightarrow\ & (CH_3)_2CO \\ & + Y_{OH} \times CH_3COCH_2O_2 \\ & + (1 - Y_{OH} - Y_{stab}) \times CO_2 + 2\,CH_3 \\ & + Y_{stab} \times H_2O_2 + (CH_3)_2CO\,.\end{aligned} \quad \text{(R7)}$$

However, 2,3-dimethyl-2-butene is a symmetric molecule with comparatively simple degradation products, mechanism development for biogenic alkenes will be considerably more complicated. Additional problems are (i) the presence of more than one double bond; (ii) formation of two Criegee intermediates in Reaction (R2) and (iii) the formation of products, which are not explicitly defined in the chemical code.

The mechanism of the terpene–ozone reactions is sufficiently well understood to allow the development of simplified oxidation schemes for a few biogenic alkenes such as α-pinene and β-pinene (Jenkin *et al.*, 2000, Winterhalder *et al.*, 2000). Although reasonably good results are obtained using the simplified approach described above, other aspects of alkene-ozone reactions still lack an explanation, e.g., the formation of pinonaldehyde as a major product in the ozonolysis of α-pinene. The major uncertainties in the evaluation of the relative importance of the ozone-alkene reactions are the large differences in the values of the rate coefficients reported in the literature.

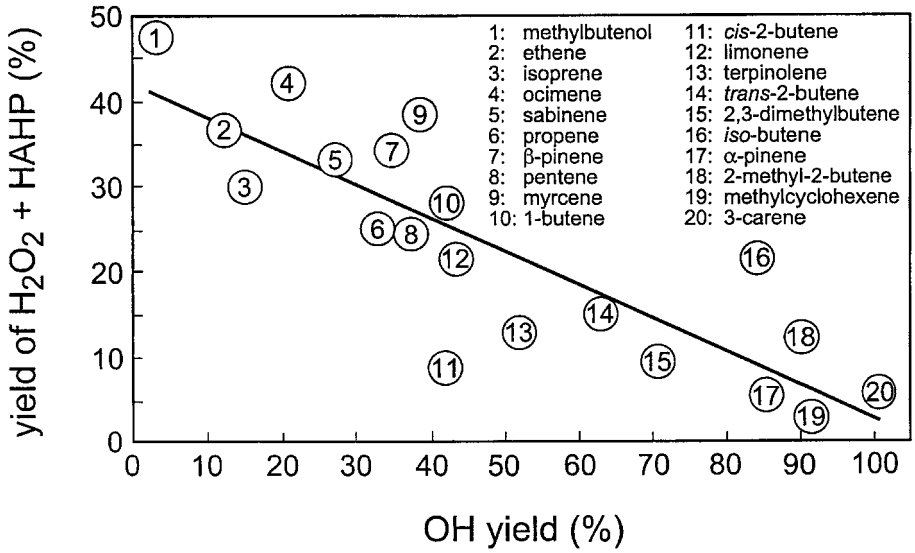

Figure 4. Yields of H_2O_2 and hydroxy alkyl hydroperoxides (HAHP) versus the OH yield for selected alkenes and terpenes.

3.3.2. *Conclusions*

In conclusion, the laboratory studies confirm that the OH radicals and hydroperoxides are formed via different energy states of the Criegee intermediate produced in the ozonolysis. Excited Criegee intermediates produce OH radicals via unimolecular decomposition, whereas stabilised Criegee intermediates react with water vapour to form (depending on structure) H_2O_2 and hydroxyalkyl hydroperoxides (HAHPs). Considerable yields of H_2O_2 and HAHP have been observed for exocyclic monoterpenes (see Figure 4), together with an associated increase in the yield of the co-product RCOR' (see Reaction (R6a)). With respect to the mechanism of the OH production (hydroperoxide channel, Reaction (R4)), extensive investigations have shown, that the co-product fragment [R′CHC(O•)R] is oxidised to an RO_2 radical, which might further influence the tropospheric oxidation capacity.

3.3.3. *Does the RACM Mechanism Predict Reactivities of Biogenic VOCs Correctly?*

Several smog chamber runs have been carried out in the outdoor simulation chamber EUPHORE in Valencia, Spain (Becker, 1996) with the biogenic alkenes isoprene, α-pinene and limonene, either as single VOCs or as additive to a three-component VOC mixture *(base mix: n*-butane, ethene, toluene) used as a simplified surrogate representative of a hydrocarbon mix in polluted ambient air. The initial carbon and NO_x concentrations of 2 ppmC and 200 ppb, respectively, as well as the proportions of the base mix VOCs were kept constant in all experiments.

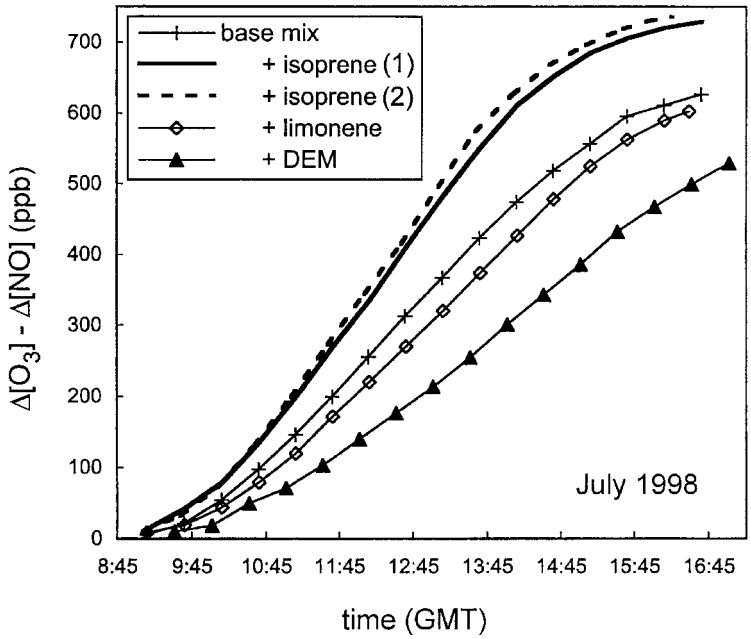

Figure 5. Comparison of $\Delta[O_3]$-Δ[NO] in a base mixture experiment and in studies with added isoprene (47.5 ppb (1), 59.6 ppb (2)), limonene (16.9 ppb) and diethoxy methane (DEM, 80.0 ppb). Base mixture: 212 ± 16 ppb *n*-butane, 208 ± 13 ppb ethene, 64 ± 4 ppb toluene.

Figure 5 shows plots of $\Delta[O_3]$-Δ[NO] against irradiation time for the surrogate base mixture and for the base mix with added isoprene, limonene or di-ethoxy methane (DEM). Whereas addition of isoprene or α-pinene (not shown in Figure 5) led to an increase of the rate of ozone formation, no such effect was observed in experiments with added limonene.

The experiments were simulated using a box model with the RACM mechanism from Stockwell *et al.*, 1997. Good agreement between simulated and measured concentration-time profiles (of ozone, NO, NO_2 and VOCs) has been obtained for the *base mix* runs and also for experiments with added α-pinene and limonene. In contrast, the ozone formation in experiments with added isoprene is under-predicted by RACM. This is also the case for experiments performed on isoprene/NO_x and α-pinene/NO_x mixtures.

The product formation from the reaction of isoprene with OH in the RACM has been modified and updated using results from recent laboratory studies (Kwok *et al.*, 1995; Chen *et al.*, 1998; Gierczak *et al.*, 1997; Ruppert and Becker, 2000). The modifications led to improvement in the agreement between simulated and measured data for the runs. The strongest influences on ozone formation were caused by the decrease of the organic nitrate yield from 0.153 to 0.08 and the increase of the reactivity of the reaction products by introducing a new product species, HCB,

representing unsaturated hydroxycarbonyls. The modifications caused the number of species and reactions in RACM to be increased by 2 and 5, respectively.

The mechanism for α-pinene was similarly extended by introducing pinonaldehyde as a separate product, which is formed in reactions of α-pinene with OH, O_3, and NO_3. Further degradation of pinonaldehyde occurs by reaction with OH and photolysis (Nozière *et al.*, 1999). In the mechanism the radical yield from the reaction of α-pinene with O_3 increased, since it was assumed that a second radical has to be formed parallel to each OH (see below). The modified mechanism, which currently contains 10 additional species and 12 additional reactions as compared to the RACM, significantly improves the simulation of the EUPHORE chamber experiments. However, it should be emphasised, that although the simulations have been improved, more mechanistic information is still required, especially for the ozonolysis and for further reactions of the products.

3.3.4. *Conclusions*

From the results obtained within the TFS project and from a comparison of the RACM degradation schemes for the three biogenic VOCs with recent experimental data, there is evidence that RACM under-predicts the reactivity of the biogenics. If this is true as the present work suggests, 3D-modelling studies using RACM could lead to erroneous conclusions with respect to

- predicting reactivity scales for biogenic VOCs,
- NO_x versus VOC sensitivity and reduction scenarios,
- anthropogenic versus biogenic influence on ozone formation,
- peak ozone levels at rural areas (e.g., levels would be under-estimated downwind of cities).

However, in the 'complexity' of the 3D model, these effects may be masked or compensated by other errors. Nevertheless, for certain applications and conditions more specific and possibly more detailed mechanisms for biogenic VOCs are required, so that the more reactive character of the biogenic VOCs compared to the anthropogenic VOCs is properly reflected. The mechanisms need to be updated frequently and evaluated against comprehensive smog chamber data sets.

3.4. REACTIONS OF SELECTED ALKOXY AND ALKYLPEROXY RADICALS

Alkoxy and alkylperoxy radicals are important intermediates in the radical chain of the tropospheric degradation of alkanes and similar compounds (e.g., ethers, alcohols). Peroxy radicals mainly react with NO forming NO_2 and an alkoxy radical, which promotes tropospheric ozone formation. The structure of the alkoxy radicals determines the relative importance of the possible loss processes, i.e., reaction with O_2, isomerisation or decomposition. The two latter pathways strengthen the overall conversion of NO to NO_2 and, therefore, the formation of ozone.

Table VII. Rate coefficients for selected alkoxy radical reactions, $T = 293$ K, $p = 37.5$ Torr (Hein *et al.*, 1998, 1999, 2000a)

Radical	Reaction	k ($cm^3\ s^{-1}$) or (s^{-1})
1-butoxy	O_2 reaction	$(1.4 \pm 0.7) \times 10^{-14}$
	isomerisation	$(3.5 \pm 2) \times 10^4$
2-butoxy	O_2 reaction	$(6.5 \pm 2) \times 10^{-15}$
	decomposition	$(3.5 \pm 2) \times 10^3$
1-pentoxy	O_2 reaction	$\leq 1.0 \times 10^{-13}$
	isomerisation	$\geq 5.0 \times 10^4$
2-pentoxy	O_2 reaction	$\leq 6.5 \times 10^{-14}$
	isomerisation	$(1.8 \pm 1) \times 10^5$
3-pentoxy	O_2 reaction	$(7.2 \pm 4) \times 10^{-15}$
	decomposition	$(5.0 \pm 2.5) \times 10^3$

3.4.1. *Rate Coefficients for the Decomposition/Isomerisation of a Series of Alkoxy Radicals and Their Reactions with O_2*

The reactions of 1-butoxy, 2-butoxy, 1-pentoxy, 2-pentoxy and 3-pentoxy radicals were studied using time-resolved and simultaneous measurement of NO_2 and OH concentrations in pulse laser-initiated oxidation studies followed by numerical simulations of the concentration profiles. Alkoxy radicals were selectively produced by excimer laser photolysis of alkylbromides at 248 nm and subsequent reaction of the corresponding alkyl radicals with O_2 and NO. All experiments were performed at 293 ± 3 and 37.5 Torr.

Alkoxy radicals show three distinct competitive reaction pathways, depending on their structure and on environmental and experimental conditions. These pathways are: (i) reaction with O_2, yielding a carbonyl compound (aldehyde or ketone) and HO_2, (ii) unimolecular decomposition, forming an aldehyde or a ketone and a shorter alkyl radical, and (iii) isomerisation (1,5-H-shift) via a 6-membered and nearly strain-free transition state.

Rate coefficients for these types of reactions were determined by parameter variation using the established FACSIMILE box model integrator (AEA Technology, U.K.), until best fits for the measured OH and NO_2 concentration time profiles were performed. Table VII summarises all rate coefficients determined for isomerisation, decomposition and reaction with O_2 for the different butoxy and pentoxy radicals investigated.

In summary, the theoretical approach as well as the experimental methods using the technique of laser pulse initiated oxidation combined with numerical simulation

of measured concentration-time profiles proved its usefulness for investigations of alkoxy radical reactions.

3.4.2. *Rate Coefficient Ratios for the Unimolecular Decomposition/Isomerisation of Selected Alkoxy Radicals and Their Reaction with O_2*

1-Butoxy, 2-butoxy, *i*-butoxy and 3-pentoxy radicals were prepared by stationary photolysis of alkyl iodide/O_2/NO/N_2 mixtures at 254 nm. The experiments were performed at 298 K, a total pressure of 760 Torr, and oxygen partial pressures between 75 and 750 Torr. Effective rate coefficient ratios $(k_{\mathrm{uni}}/k_{\mathrm{O_2}})_{\mathrm{eff}}$ were derived from the product distributions as measured by long-path IR absorption using a FT-IR spectrometer. For example, acetaldehyde and butanone are the products formed in the dissociation (k_{dis}) and the O_2 reaction ($k_{\mathrm{O_2}}$), respectively, of 2-butoxy radicals. For 2-butoxy, $k_{\mathrm{dis}}/k_{\mathrm{O_2}}$ was derived from experiments at different oxygen pressures, based on the following equation:

$$k_{\mathrm{dis}}/k_{\mathrm{O_2}} = ([\mathrm{CH_3CHO}] \times [\mathrm{O_2}])/(2 \times \Delta[\mathrm{butanone}]) \,. \quad (1)$$

The factor of 2 arises due to the formation of one molecule of acetaldehyde directly in the dissociation reaction of 2-butoxy radicals and a second from the further reaction of the second dissociation product, C_2H_5. A nearly complete product analysis was performed, and small corrections were made for the formation of ethyl nitrate, ethyl nitrite and products of the reaction of acetaldehyde with OH radicals (PAN, formaldehyde). In the case of 1-butoxy radicals, the isomerisation products (hydroxycarbonyls) could not be quantified, and the determination of $k_{\mathrm{iso}}/k_{\mathrm{O_2}}$ is based solely on the analysis of butanal, including corrections for the formation of 1-butyl nitrate and 1-butyl nitrite, which reduce the yield of 1-butoxy radicals.

For all alkoxy radicals studied by this method, the ratios $k_{\mathrm{uni}}/k_{\mathrm{O_2}}$ as defined by Equation (1) and equivalent expressions for the other alkoxy radicals showed a linear increase with the oxygen partial pressure by 40–115% in the range 75–750 Torr O_2. This increase depends on the type of the alkoxy radical, which is summarised in Table VIII. It should be possible to reduce the error limits in the near future by a more complete analysis of the side products. The values calculated here for atmospheric conditions (298 K, 150 Torr O_2, total pressure 750 Torr, M=$N_2 + O_2$) are in reasonable agreement with experimental data of Carter *et al.* (1979), Cox *et al.* (1981), Blitz *et al.* (1998), Hein *et al.* (1998, 1999, 2000a), and Atkinson *et al.* (1995), as well as with semi-empirical estimates of Atkinson (Atkinson, 1997), and *ab-initio* calculations of k_{dis} of Somnitz and Zellner (2000a, b, c). For *i*-butoxy radicals, no other experimental data are available. Agreement with the value from the estimation method of Atkinson is achieved only when the JPL value of the heat of formation of the *i*-propyl radical (DeMore *et al.*, 1997) is used in this estimation rather than the more commonly accepted value of Atkinson *et al.* (1999). The O_2 dependence of $k_{\mathrm{uni}}/k_{\mathrm{O_2}}$ observed in this work is most easily explained by the formation of 10–20% of chemically activated alkoxy radicals in the reaction $RO_2 + NO$ ($RO + NO_2$. Recently, a similar effect has been described by other research groups

Table VIII. Dependence of $(k_{uni}/k_{O_2})_{eff}$ on the O_2 concentration at 298 K for several alkoxy radicals (Libuda *et al.*, 2000; Shestakov *et al.*, 2000); ($(k_{uni}/k_{O_2})_{eff} = A + B \times [O_2]$, see text)

Radical	A (cm^3 $molecule^{-1}$)	B	$(k_{uni}/k_{O_2})_{eff}$ at 150 Torr O_2 and 600 Torr N_2 (molecule cm^3)	k_{uni}/k_{O_2} [a] at 750 Torr (O_2 + N_2) (Hein *et al.*, see Table IV) (molecule cm^3)	Primary products of RO (750 Torr air, 298 K)
1-butoxy	1.34×10^{19}	0.26	$(1.8 \pm 0.6) \times 10^{19}$	1.0×10^{19}	butanal (22%) 4-hydroxy butanal (78%)
2-butoxy	2.4×10^{18}	0.13	$(3.0 \pm 0.6) \times 10^{18}$	2.7×10^{18}	2-butanone (63%) acetaldehyde (37%)
i-butoxy	5.2×10^{18}	0.20	$(6.2 \pm 1.2) \times 10^{18}$	–	*iso*-butanal (45%) formaldehyde (55%)
3-pentoxy	2.7×10^{18}	0.16	$(3.6 \pm 0.7) \times 10^{18}$	3.2×10^{18}	3-pentanone (58%) acetone (52%)

[a] Converted from experimental conditions (37.5 Torr, 293 K) to 750 Torr, 298 K, using calculated activation energies and pressure fall-off data from Somnitz and Zellner (2000a, b).

Table IX. NOCON factors experimentally obtained for selected linear, branched, cyclic and oxygenated VOCs (Hein *et al.*, 2000b)

Chain length	$NOCON_{linear}$	$NOCON_{bran,\ cyc}$	$NOCON_{oxy}$
1	2.0		
2	2.0		2.0
3	2.0		1.5, 1.8
4	3.1		
5	3.7	2.9, 3.5	
6	4.3	2.7, 3.0, 3.1	
7	5.6		
8	5.9		

for halogenated and hydroxylated alkoxy radicals (Wallington *et al.*, 1996; Orlando *et al.*, 1998). In Table VIII, the results from the stationary method are compared with rate coefficient ratios derived from the individual rate coefficients k_{uni} and k_{O_2} as determined by Hein *et al.* (see Tables VII and VIII), demonstrating the good agreement of the two data sets obtained by completely different methods. This is shown in the last column of Table VIII for the alkoxy radicals investigated, both unimolecular transformation and reaction with O_2 are of comparable importance under tropospheric conditions.

3.4.3. *Determination of NOCON Factors*

In a second set of experiments, the NOCON factors (Hein *et al.*, 1998, 1999, 2000a), i.e., the ratio $\Delta[NO_2]/\Delta[VOC]$, the amount of NO_2 produced per molecule VOC oxidised, of a variety of linear, branched, cyclic and oxygenated VOCs were directly measured. The NOCON factors as a function of chain length of the VOCs investigated are summarised in Table IX. NOCON factors obtained for the linear VOCs increase with increasing chain length, indicating that isomerisation and decomposition are the dominant reaction pathways for larger VOC (more than 4 C atoms), whereas reaction with O_2 is the main degradation pathway for smaller VOC (1–3 C atoms). NOCON factors of the branched and cyclic VOCs are in the range 2.7–3.5, those of alcohols in the range 1.5–2.0. Since their oxidation mechanisms include one NO/NO_2 conversion cycle less, their NOCON factors are generally smaller than those of non-oxygenated VOC.

In conclusion, NOCON factors offer the possibility to concentrate the different possible reaction pathways of alkoxy radicals in one parameter. Accordingly, explicit knowledge of complete oxidation mechanisms is not always necessary for the description of atmospheric chemical systems.

3.4.4. *Investigation of the Chemistry of 2-Butylperoxy Radicals in the Presence of NO_x*

The chemical processes leading to the formation of ozone proceed via the conversion of NO to NO_2 by peroxy radicals (RO_2). For the determination of the ozone forming potential of a certain hydrocarbon, it is therefore important to know the accurate number of peroxy radicals produced during the oxidative degradation process of this species.

This number depends on two factors: the formation yield (α) of organic nitrates ($RONO_2$) and the production rate of RO_2 during the subsequent reactions of the alkoxy radical (RO). This rate is given by the ratio of the rate coefficients of isomerisation and decomposition of the RO radical to the rate coefficient of its reaction with O_2. Both factors were obtained for the 2-butylperoxy radical within the project.

The present value of $(1.9 \pm 1.0) \times 10^{18}$ cm^{-3} for $(k_{\text{isom}} + k_{\text{dec}})/k_{O_2}$ is comparable to the literature data of Libuda *et al.* (2000, $(3.0 \pm 0.6) \times 10^{18}$ cm^{-3}), Hein *et al.* (1998, $(3.0 \pm 0.6) \times 10^{18}$ cm^{-3}) and Atkinson (1997, 4.6×10^{18} cm^{-3}). The α value of (0.089 ± 0.007) determined here is in excellent agreement with that of Libuda *et al.* (2000, see also Table IX). This value indicates that 48% of the 2-butyloxy radicals will decompose. Accordingly, about 1.3 RO_2 radicals are formed in the whole degradation chain of the 2-butyl radical.

3.4.5. *Conclusions*

Within the TFS/LT3 programme, the database of the reaction pathways of alkoxy and alkylperoxy radicals in the atmosphere was significantly extended. A couple of reactions were studied for the first time. In addition, a number of reactions were re-investigated. The present results together with already existing literature data offer the revision of chemical modules used for CT models in order to yield a better description of VOC degradation chains in the atmosphere.

3.5. ENVIRONMENTAL CHAMBER EXPERIMENTS

Within the TFS programme, a new outdoor simulation chamber (*SAPHIR*) at the Research Center Jülich was constructed (Wahner and Dorn, 2000). Though the chamber was not completed before the TFS project was finished, a couple of experimental and theoretical studies, focused on the chemical and physical characterisation of the chamber, were carried out. These pre-investigations mainly concentrated on the correct description of the radical budget in future experiments, which is one of the most sensitive parameters for the successful interpretation of smog chamber studies. Detailed information about the SAPHIR chamber can be obtained from the world wide web (FZ Jülich, 2000).

3.5.1. *Characterisation of a New Simulation Chamber*

3.5.1.1. *Laser-Induced Self-Production of OH Radicals Measured by Long Path Laser Absorption Measurements.* When multiple-reflection cells are used for the measurement of OH radicals by long-path UV absorption spectroscopy, the probability of OH self-production (Reactions (R1) and (R2)) in the enhanced UV laser radiation field within the cell cannot be excluded *a priori*.

$$O_3 + h\nu\ (\lambda_{\text{laser}} = 308\ \text{nm}) \rightarrow O^1D + O_2 \tag{R8}$$

$$O^1D + H_2O \rightarrow OH + OH\,. \tag{R9}$$

Experiments were performed to investigate the effect for laser-induced self-production of OH using a folded long-path absorption instrument (Hausmann *et al.*, 1997).

Laser-induced OH formation by the Reactions (R8) and (R9) at different levels of ozone was investigated in the Jülich Atmosphere Simulation Chamber *SAPHIR*. Due to delays in completion of the final chamber construction the measurements were performed within the outer protection cover of the chamber and not within the Teflon walls which are currently being erected.

All experiments were performed using a total light path of 1103 m, corresponding to 56 passes through the White optics mounted within the chamber. The composition of the air within the chamber corresponded to outside air. The ozone mixing ratio was varied from ambient conditions (36 ppb) up to about 2000 ppb.

As already demonstrated by Gerlach (1991), the concentration of laser-induced OH increases proportional to ozone. However, the measurements showed that at ozone mixing ratios less than 400 ppb the concentration of OH remained below the detection limit of the instrument which varied between $(1.5–2.5) \times 10^6$ OH radicals per cm^3 (see Figure 6).

Nevertheless these experiments will be repeated after completion of *SAPHIR* although most of the planned chamber experiments will be performed at considerably lower ozone mixing ratios.

3.5.1.2. *OH Formation on the Chamber Walls.* Model studies have been conducted to study the influence of wall reactions on the chemistry in the *SAPHIR* chamber. One of the potentially most important reactions is the light-induced production of OH radicals (Carter *et al.*, 1995). Following the parametrisation of the OH source strength as function of the radiation and adopting a simple scaling law for the dependence on the chamber volume V and the wall surface area F the volume source strength can be described by (Bluhm, 1998):

$$S_0(\text{OH}) = 3.08 \times 10^{24}\ \text{cm}^{-2}\ F/V\ j(\text{NO}_2) \exp(-9556.16\ K/T). \tag{2}$$

Box model calculations for stationary concentrations of short-lived compounds as a function of the forcing parameters (pressure, temperature, and radiation) and the

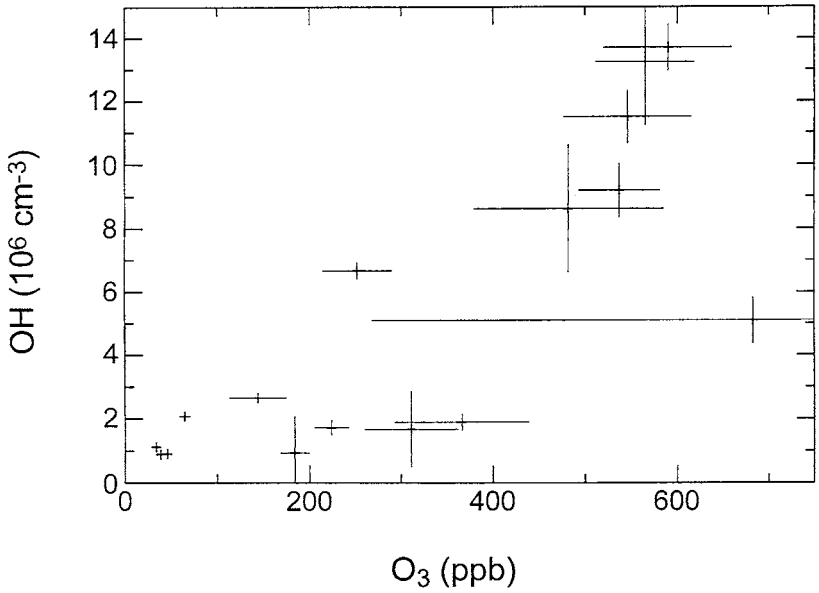

Figure 6. Dependence of the laser-induced OH concentration on the mixing ratio of ozone in the simulation chamber *SAPHIR*.

concentrations of longer-lived precursors and reaction partners were undertaken to explore the possible impact on the OH concentration. The two-dimensional contour plot illustrated in Figure 7 shows the dependence of the OH concentration on the mixing ratio of NO_2 and on S(OH). If $S(OH)/S_0(OH) > 1$, the wall source must be taken into account. The estimation of $S_0(OH)$ in Equation (2) is highly uncertain, thus a measurement in the *SAPHIR* chamber is a necessary prerequisite of a quantitative comparison between model and experiment.

Other wall processes, in particular losses of ozone, N_2O_5, HNO_3 and NO_2, are associated with lifetimes of typically more than a day (Mentel and Wahner, 1996; Mentel and Sohn, 1997). For the modelling of short-lived species in chamber studies under experimental constraints for the longer lived compounds, these processes do not need to be considered.

4. Summary and Conclusions

The TFS/LT3 programme yielded important results from the experimental investigation of complex chemical processes related to tropospheric photochemistry. A substancial number of rate coefficients for elementary steps were determined. Intensive product studies of the tropospheric degradation of selected aromatic, oxygenated and biogenic VOC were performed. For several oxygenated organic compounds, explicit reaction mechanisms were constructed and tested against experimental data. In total, the results of the present work significantly increase the chemical data base necessary for the further development and improvement of

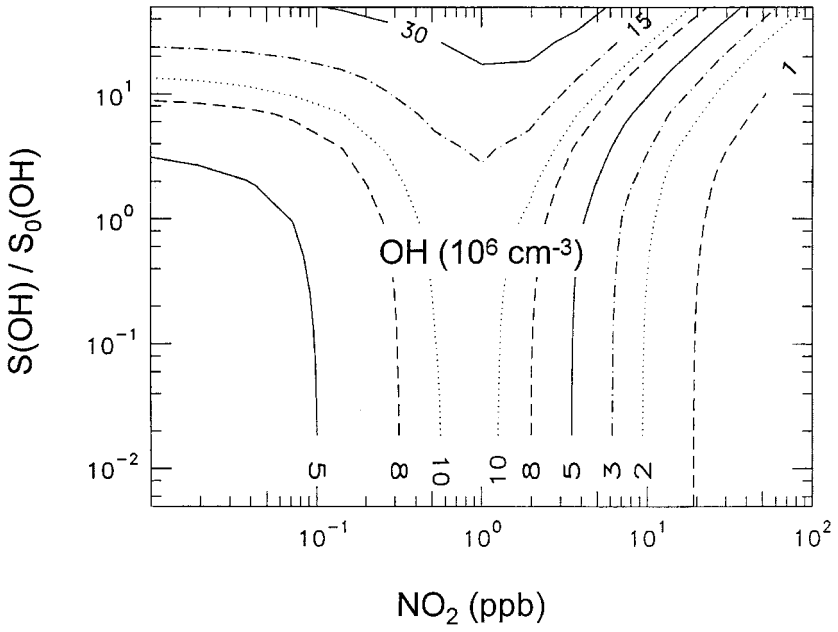

Figure 7. Contour plot of OH as function of NO_2 and the source strength S(OH) of the OH wall source. S_0(OH) is the estimated value for *SAPHIR* based on literature data (see Equation (2)).

chemical modules used in chemistry transport models (CTM) with the final goal of more precise ozone prognosis on regional and global levels.

Acknowledgements

Support for this research was provided by the German Bundesministerium für Bildung und Forschung (BMBF), project 'Förderschwerpunkt Troposphärenforschung (TFS)', contract 07TFS30.

References

Atkinson, R., 2000: Atmospheric chemistry of VOCs and NO_x, *Atmos. Environ.* **34**, 2063–2101.

Atkinson, R., Baulch, D. L., Cox, R. A., Hampson Jr., R. F., Kerr, J. A., Rossi, M. J., and Troe, J., 1999: Evaluated kinetic and photochemical data for atmospheric chemistry, organic species: Supplement VII, *J. Phys. Chem. Ref. Data* **28**, 191–393.

Atkinson, R., 1997: Gas-phase tropospheric chemistry of volatile organic compounds: 1. Alkanes and alkenes, *J. Phys. Chem. Ref. Data* **26**, 215–290.

Atkinson, R., Kwok, E. S. C., Arey, J., and Aschmann, S. M., 1995: Reactions of alkoxyl radicals in the atmosphere, *Faraday Discuss.* **100**, 23–37.

Atkinson, R., 1994: Gas-phase tropospheric chemistry of organic compounds, *J. Phys. Chem. Ref. Data*, Monograph 2.

Barnes, I. and Donner, B., 2000: Wirkung reformulierter un alternativer Kraftstoffe auf die Bildung von Photooxidantien in urbaner Luft, in K. H. Becker (ed.), *TFS-LT3 Annual Report 1999*, University of Wuppertal, Germany, pp. 233–241.

Barnes, I. and Wenger, J. (eds.), 1998: EUPHORE Report 1997, University of Wuppertal, Wuppertal, Germany.

Barnes, I., Becker, K. H., and Mihalopoulos, N., 1994: An FTIR study of the photooxidation of dimethyl disulfide, *J. Atmos. Chem.* **18**, 267–289.

Bauerle, S. and Moortgat, G. K., 1999: Absorption cross-sections of $HOCH_2OOH$ vapor between 205 and 360 nm at 298 K, *Chem. Phys. Lett.* **309**, 43–48.

Becker, K. H., Freitas Dinis, C. M., Geiger, H., and Wiesen, P., 1999a: The reactions of OH radicals with di-*i*-propoxymethane and di-*sec*-butoxymethane: Kinetic measurements and structure activity relationships, *Phys. Chem. Chem. Phys.* **1**, 4721–4726.

Becker, K. H., Dinis, C., Geiger, H., and Wiesen, P., 1999b: Kinetics of the reaction of OH with di-*n*-butoxymethane (DBM) in the range 298-710 K, *Chem. Phys. Lett.* **300**, 460–464.

Becker, K. H. (ed.), 1998: Influence of fuel formulation on atmospheric reactivity of exhaust gases (INFORMATEX), Final Report of the EC Project ENV4-CT95-0015, Wuppertal, Germany.

Becker, K. H. (ed.), 1996: The European photoreactor EUPHORE, Final Report of the EC Project EV5V-CT92-0059, Wuppertal, Germany.

Becker, K. H., Bechara, J., and Brockmann, K. J., 1993: Studies on the formation of H_2O_2 in the ozonolysis of alkenes, *Atmos. Environ.* **27A**, 57–61.

Becker, K. H., Brockmann, K. J., and Bechara, J., 1990: Production of hydrogen peroxide in forest air by reaction of ozone with terpenes, *Nature* **346**, 256–258.

Blitz, M. A., Pilling, M. J., and Seakins, P. W., 1998: Absolute rate constants for some butoxy radical reactions, *Proceedings of the 15th International Symposium on Gas Kinetics,* Contribution no. D19, Bilbao, Spain.

Bluhm, H., 1998: Modelluntersuchungen zur Chemie von Spurenstoffen in einer Atmosphärensimulationskammer: Sensitivitätsstudie zum Einfluß von Reaktionen an der Kammeroberfläche, Diploma Thesis, University of Cologne, Germany.

Bohn, B., Elend, M., and Zetzsch, C., 2000: Abbaumechanismen von Aromaten nach Anlagerung von OH und ihr Einfluß auf die Kreisläufe von HO_x unter Bildung von Photooxidantien, in K. H. Becker (ed.), *TFS-LT3 Annual Report 1999*, University of Wuppertal, Germany, pp. 217–227.

Bohn, B. and Zetzsch, C., 1999: Gas-phase reaction of the OH-benzene adduct with O_2: Reversibility and secondary formation of HO_2, *Phys. Chem. Chem. Phys.* **1**, 5097–5107.

Brown, P. N., Byrne, G. D., and Hindmarsh, A. C., 1989: VODE: A variable-coefficient ODE solver, *J. Sci. Stat. Comput.* **10**, 1038–1051.

Calvert, J. G., Atkinson, R., Kerr, J. A., Madronich, S., Moortgat, G. K., Wallington T. J., and Yarwood, G., 2000: *The Mechanisms of Atmospheric Oxidation of the Alkenes*, Oxford University Press, Inc., New York, U.S.A.

Carter, W. P. L., Luo, D., Malkina, I. L., and Pierce, J.A., 1995: Environmental chamber studies of atmospheric reactivities of volatile organic compounds. Effects of varying chamber and light source, Final Report to National Renewable Energy Laboratory, Contract No. XZ-2-12075, Riverside, CA, U.S.A.

Carter, W. P. L., 1994: Development of ozone reactivity scales for volatile organic compounds, *J. Air Waste Manage. Assoc.* **44**, 881–899.

Carter, W. P. L., Lloyd, A. C., Sprung, J. L., and Pitts Jr., J. N., 1979: Computer modeling of smog chamber data: Progress in validation of a detailed mechanism for the photooxidation of propene and *n*-butane in photochemical smog, *Int. J. Chem. Kinet.* **11**, 45–101.

Chen, X., Hulbert, D., and Shepson, P. B., 1998: Measurement of the organic nitrate yield from OH reaction with isoprene, *J. Geophys. Res.* **103**, 25563–25568.

Cox, R. A., Patrick K. F., and Chant, S. A., 1981: Mechanism of atmospheric photooxidation of organic compounds. Reactions of alkoxy radicals in oxidation of *n*-butane and simple ketones, *Environ. Sci. Technol.* **15**, 587–592.

DeMore, W. B., Sander, S. P., Golden, D. M., Hampson, R. F., Kurylo, M. J., Howard, C. J., Ravishankara, A. R., Kolb, C. E., and Molina, M. J., 1997: Chemical kinetics and photochemical data for use in stratospheric modeling, *JPL Publication* **97** (4), Jet Propulsion Laboratory, Pasadena, CA, U.S.A.

Derwent, R. G., Jenkin, M. E., Saunders, S. M., and Pilling, M. J., 1998: Photochemical ozone creation potentials for organic compounds in northwest Europe calculated with a master chemical mechanism, *Atmos. Environ.* **32**, 2429–2441.

Etzkorn, T., Klotz, B., Sørensen, S., Patroescu, I. V., Barnes, I., Becker, K. H. and Platt, U., 1999: Gas-phase absorption cross sections of 24 monocycle aromatic haydrocarbons in the UV and IR spectral ranges, *Atmos. Environ.* **33**, 525–540.

FZ Jülich, 2000: http://www.fz-juelich.de/icg/icg3/saphir/saphir_de.html (periodically updated).

Gear, C. W., 1971: Numerical initial value problems in ordinary differential equations, *Prentice-Hall Series in Automatic Computation* Vol. 17, Prentice-Hall, Englewood Cliffs, U.S.A.

Geiger, H. and Becker, K. H., 1999: Degradation Mechanisms of dimethoxymethane and dimethoxyethane in the presence of NO_x, *Atmos. Environ.* **33**, 2883–2892.

Geiger, H., Maurer, T., and Becker, K. H., 1999: OH-Initiated Degradation Mechanism of 1,4-Dioxane in the Presence of NO_x, *Chem. Phys. Lett.* **314**, 465–471.

Gerlach, R., 1991: Aufbau und Charakterisierung eines Vielfachreflexionssystems zur Messung von Hydroxyl-Radikalen in der Troposphäre, PhD Thesis, University of Cologne, Germany.

Gierczak, T., Burkholder, J. B., Talukdar, R. K., Mellouki, A., Barone, S. B., and Ravishankara, A. R., 1997: Atmospheric fate of methyl vinyl ketone and methacrolein, *J. Photochem. Photobiol. A: Chem.* **110**, 1–10.

Grossmann, D., 1999: Die Gasphasenozonolyse von Alkenen in Gegenwart von Wasserdampf als Quelle für Wasserstoffperoxid und organische Peroxide in der Atmosphäre, PhD Thesis, Johannes Gutenberg University, Mainz, Germany.

Grossmann, D., Valverde-Canossa, J., Neeb, P., and Moortgat, G. K., 2000: in preparation.

Hass, H., 2000: Untersuchungen zum atmosphärischen Abbau von alternativen Kraftstoffen und Kraftstoffzusätzen, in K. H. Becker (ed.), *TFS-LT3 Annual Report 1999*, University of Wuppertal, Germany, pp. 259–269.

Hatakeyama, S., Kobayashi, H., and Akimoto, H., 1984: Gas-phase oxidation of SO_2 in the ozone-olefin reactions, *J. Phys. Chem.*, **88**, 4736–4739.

Hausmann, M., Brandenburger, U., Brauers, T., and Dorn, H.-P., 1997: Detection of tropospheric OH radicals by long-path differential-optical-absorption spectroscopy: Experimental setup, accuracy and precision, *J. Geoph. Res.* **102**, 16011–16022.

Hein, H., Hoffmann, A., and Zellner R., 1998: Direct investigation of reactions of 2-butoxy radicals using laser-initiated oxidation: Reaction with O_2 and unimolecular decomposition at 293 K and 50 mbar, *Ber. Bunsenges. Phys. Chem.* **102**, 1840–1849.

Hein, H., Hoffmann, A., and Zellner R., 1999: Direct investigations of reactions of 1-butoxy and 1-pentoxy radicals using laser pulse initiated oxidation: reaction with O_2 and isomerisation at 293 K and 50 mbar, *Phys. Chem. Chem. Phys.* **1**, 3743–3752.

Hein, H., Somnitz, H., Hoffmann, A., and Zellner, R., 2000a: A combined experimental and theoretical investigation of the reactions of 3-pentoxy radicals: Reaction with O_2 and unimolecular decomposition, *Z. Phys. Chem.* **214**, 449–471.

Hein, H., Hoffmann, A., and Zellner R., 2000b: in preparation.

Hoffmann, A., Mörs, V., and Zellner, R., 1992: A novel laser-based technique for the time-resolved study of integrated hydrocarbon oxidation mechanisms, *Ber. Bunsenges. Phys. Chem.* **96**, 437–440.

Jenkin, M. E., Saunders, S. M., and Pilling, M. J., 1997: The Tropospheric degradation of volatile organic compounds: A protocol for mechanism development, *Atmos. Environ.* **31**, 81–104.

Jenkin, M. E., Shallcross, D. E., and Harvey J. N., 2000: Development and application of a possible mechanism for the generation of *cis*-pinic acid from the ozonolysis of α- and β-pinene, *Atmos. Environ.* **34**, 2837–2850.

Klotz, B., Barnes, I., Becker, K. H., and Golding, B. T., 1997: Atmospheric chemistry of benzene oxide/oxepin, *J. Chem. Soc., Faraday Trans.* **93** 1507–1516.

Klotz, B., Sørensen, S., Barnes, I., Becker, K. H., Etzkorn, T., Volkamer, R., Platt, U., Wirtz, K., and Martín-Reviejo, M., 1998a: Atmospheric oxidation of toluene in a large-volume outdoor photoreactor: In situ determination of ring-retaining products, *J. Phys. Chem. A* **102,** 10289–10299.

Klotz, B., Barnes, I., and Becker, K. H., 1998b: New Results on the atmospheric photooxidation of simple alkylbenzenes, *Chem. Phys.* **231**, 289–301.

Klotz, B., Barnes, I., and Becker, K. H., 1999: Kinetic study of the gas-phase photolysis and OH radical reaction of E,Z- and E,E-2,4-hexadienedial, *Int. J. Chem. Kinet*. **31,** 689–697.

Klotz, B., Barnes, I., Becker, K. H., and Golding, B. T., 2000: Atmospheric chemistry of toluene-1,2-oxide/2-methyloxepin, *Phys. Chem. Chem. Phys*. **2**, 227–235.

Klotz, B., Graedler, F., Sørensen, S., Barnes, I., and K. H. Becker, K. H., 2001: A kinetic study of the atmospheric photolysis of α-dicarbonyls, *Int. J. Chem. Kinet* **33**, 9–20.

Knispel, R., Koch, R., Siese, M., and Zetzsch, C., 1990: Adduct formation of OH radicals with benzene, toluene, and phenol and consecutive reactions of the adducts with NO_x and O_2, *Ber. Bunsenges. Phys. Chem.* **94**, 1375–1379.

Kurtenbach, R., Ackermann, R.,. Geyer, A., Gomes, J.A.G., Lörzer, J. C., Niedojadlo, A. Platt, U., and Becker, K. H., 2000: Auswirkungen von Kraftfahrzeug emissionen, insbesondere von Aromaten und deren Abbauprodukten, in der urbanen Atmosphäre, in K. H. Becker (ed.), *TFS-LT3 Annual Report 1999*, University of Wuppertal, Germany, pp. 207–214.

Kwok, E. S. C., Atkinson, R., and Arey, J., 1995: Observation of hydroxycarbonyls from the OH radical-initiated reaction of isoprene, *Environ. Sci. Technol.* **29**, 2467–2469.

Libuda, G., Shestakov, O., Theloke, J., and Zabel, F., 2000: in preparation.

Ma, S., Barnes, I., and Becker, K. H., 1998: Atmospheric degradation of glycidaldehyde: Photolysis and reaction with OH radicals, *Environ. Sci. Technol.* **32**, 3515–3521.

Madronich, S., 1987: Photodissociation in the atmosphere; 1. Actinic flux and the effects on ground reflections and clouds, *J. Geophys. Res*. **92**, 9740–9752.

Maurer, T., Geiger, H., Barnes, I., Becker, K. H., and Thüner, L. P., 2000: Kinetic, mechanistic and modeling study of the OH radical initiated oxidation of di-*n*-butoxy methane (DNBM), *J. Phys. Chem. A* **104**, 11087–11094.

Maurer T., Hass, H., Barnes, I., and Becker, K. H., 1999: Kinetic and product study of the atmospheric photooxidation of 1,4-dioxane and its main reaction product ethylene glycol diformate, *J. Phys. Chem. A* **103**, 5032–5039.

Mentel, Th. F. and Sohn, M., 1997: Private communication.

Mentel, Th. F. and Wahner, A., 1996, A large reaction chamber for nighttime atmospheric chemistry: Design and characteristics of the reaction chamber, *Reports of the Research Center Jülich*, JÜL-3196, Jülich, Germany.

Neeb, P., Horie, O., and Moortgat, G. K., 1996: Formation of secondary ozonides in the gas-phase ozonolysis of simple alkenes, *Tetrahedron Lett.* **37**, 9297–9300.

Neeb, P., Sauer, F., Horie, O., and Moortgat, G. K., 1997: Formation of hydroxymethyl hydroperoxide and formic acid in alkene ozonolysis in the presence of water vapour, *Atmos. Environ.* **31**, 1417–1423.

Neeb, P., Horie, O., and Moortgat, G. K., 1998: The ethene-ozone reaction in the gas phase, *J. Phys. Chem. A* **102**, 6778–6785.

Neeb, P. and Moortgat, G. K., 1999: Formation of OH radicals in the gas-phase reaction of propene, isobutene, and isoprene with O_3: Yields and mechanistic implications, *J. Phys. Chem. A* **103**, 9003–9012.

Olariu, R. I., Barnes, I., Becker, K. H., and Klotz, B. K., 2000: Rate coefficients for the gas-phase reaction of OH radicals with selected dihydroxybenzenes and benzoquinones, *Int. J. Chem. Kinet*., 696–702.

Orlando, J. J., Tyndall, G. S., Bilde, M., Ferronato, C., Wallington, T. J., Vereecken, L., and Peeters, J., 1998: Laboratory and theoretical study of the oxy radicals in the OH- and Cl-initiated oxidation of ethene, *J. Phys. Chem. A* **102**, 8116–8123.

Paulson, S. E., Chung, M., and Hassam A.S., 1999: OH Radical formation from the gas-phase reaction of ozone with terminal alkenes and the relationship between structure and mechanism, *J. Phys. Chem. A* **103**, 8125–8138.

Platz, J., Christensen, L. K., Sehested, J., Nielsen, O. J., Wallington, T. J., Sauer, C., Barnes, I., Becker, K. H., and Vogt, R., 1998: Atmospheric chemistry of 1,3,5-Trioxane: UV Spectra of c-$C_3H_5O_3$(•) and (c-$C_3H_5O_3$)O_2(•) radicals, kinetics of the reactions of (c-$C_3H_5O_3$)O_2(•) radicals with NO and NO_2, and atmospheric fate of the alkoxy radical (c-$C_3H_5O_3$)O(•), *J. Phys. Chem. A* **102**, 4829–4838.

Ruppert, L. and Becker, K. H., 2000: A product study of the OH radical-initiated oxidation of isoprene: Formation of C_5-unsaturated diols, *Atmos. Environ.* **34**, 1529–1542.

Rickard A. R., Johnson, D., McGill, C. D., and Marston G., 1999: OH yields in the gas-phase reactions of ozone with alkenes,, *J. Phys. Chem. A* **103**, 7656–7664.

Sauer, C. G., Barnes, I., Becker, K. H., Geiger, H., Wallington, T. J., Christensen, L. K., Platz, J., and Nielsen, O. J., 1999a: Atmospheric chemistry of 1,3-dioxolane: Kinetic, mechanistic, and modeling study of OH radical initiated oxidation, *J. Phys. Chem. A* **103**, 5959–5966.

Sauer, F., Schäfer, C., Neeb, P., Horie, O., and Moortgat, G. K., 1999: Formation of hydrogen peroxide in the ozonolysis of isoprene and simple alkenes under humid conditions, *Atmos. Environ.* **33**, 229–241.

Seefeld, S. and Stockwell, W. R., 1999: First-order sensitivity analysis of models with time-dependent parameters: an application to PAN and ozone, *Atmos. Environ.* **33**, 2941–2955 (and references therein).

Shestakov, O., Libuda, H. G., and Zabel, F., 2000: in preparation.

Somnitz, H. and Zellner, R., 2000a: Theoretical studies of unimolecular reactions of C2-C5 alkoxy radicals. Part I. Ab initio molecular orbital calculations, *Phys. Chem. Chem. Phys.* **2**, 1899–1906.

Somnitz, H. and Zellner, R., 2000b: Theoretical studies of unimolecular reactions of C2-C5 alkoxy radicals. Part II. RRKM dynamical calculations, *Phys. Chem. Chem. Phys.* **2**, 1907–1919.

Somnitz, H. and Zellner, R., 2000c: Theoretical studies of unimolecular reactions of C2-C5 alkoxy radicals. Part III. A microscopic structure activity relationship (SAR), *Phys. Chem. Chem. Phys.* **2**, 4319–4325.

Stockwell, W. R., Geiger, H., and Becker, K.H., 2001: Estimation of incremental reactivities for multiple day scenarios: An application to ethane and dimethyoxymethane, *Atmos. Environ.* **35**, 929–939.

Stockwell, W. R., Kirchner, F., Kuhn, M., and Seefeld, S., 1997: A new mechanism for regional atmospheric chemistry modeling, *J. Geophys. Res.* **102**, 25847–25879.

Stockwell, W.R., Middleton P., Chang J.S., and Tang X., 1990: The second generation regional acid deposition model chemical mechanism for regional air quality modeling, *J. Geophys. Res.* **95**, 16343–16367.

Thamm, J., Wolff, S., Turner, W. V., Gäb, S., Thomas, W., Zabel, F., Fink, E. H., and Becker, K. H., 1996: Proof of the formation of hydroperoxymethyl formate in the ozonolysis of ethene: synthesis and FT-IR spectra of the authentic compound, *Chem. Phys. Lett.* **258**, 155–158.

Thüner, L. P., Barnes, I., Maurer, T., Sauer, C. G., and Becker, K. H., 1999: Kinetic and product study of the atmospheric photooxidation of 1,4-dioxane and its main reaction product ethylene glycol diformate, *J. Phys. Chem. A* **103**, 5032–5039.

Wahner, A. and Dorn, H.-P., 2000: Untersuchung der OH-Radikalkonzentrations-Zeitprofile in einer Tageslicht-Atmosphärenkammer mittels gefalteter Laser-Langwegabsorption, in K. H. Becker (ed.), *TFS-LT3 Annual Report 1999*, University of Wuppertal, Germany, pp. 323–332.

Wallington, T. J., Hurley, M. D., Fracheboud, J. M., Orlando, J. J., Tyndall, G. S., Sehested, J., Møgelberg, T. E., and Nielsen, O. J., 1996: Role of excited CF_3CFHO radicals in the atmospheric chemistry of HFC-134a, *J. Phys. Chem.* **100**, 18116–18122.

Winterhalter, R., Neeb, P., Grossmann, D., Kolloff, A., Horie, O., and Moortgat, G. K., 2000: Products and mechanism of the gas phase reaction of ozone with β-pinene, *J. Atm. Chem.* **35**, 165–197.